Candida albicans enhances the progression of oral squamous cell cancrinoma *in vitro* and *in vivo*

Authors

Vadovics M[1,2], Igaz N[2,3], Alföldi R[4], Rakk D[1,2], Veres É[1,2], Szücs B[1], Horváth M[1], Tóth R[1], Szücs A[1], Horváth P[5], Tiszlavicz L[6], Vágvölgyi C[1], Nosanchuk JD[7], Szekeres A[1], Kiricsi M[3], Puskás LG[4], Gácser A[1,8]

Affiliations

1 Department of Microbiology, University of Szeged, Közép fasor 52, 6726, Szeged, Hungary.

2 Doctoral School of Biology, University of Szeged, Közép fasor 52, 6726, Szeged, Hungary.

3 Department of Biochemistry and Molecular Biology, Faculty of Science and Informatics, University of Szeged, Közép fasor 52, 6726, Szeged, Hungary.

4 AstridBio Technologies Ltd., Wimmer Fülöp 1, H6728 Szeged, Hungary

5 Synthetic and System Biology Unit, Biological Research Centre (BRC), Szeged H-6726, Hungary.

6 Department of Pathology, University of Szeged, Állomás u. 2, 6725, Szeged, Hungary.

7 Department of Medicine; Division of Infectious Diseases; Department of Microbiology and Immunology; Albert Einstein College of Medicine ; Bronx , NY , USA.

8 MTA-SZTE Lendület Mycobiome Research Group, University of Szeged, Szeged, Hungary.

Corresponding author

Gácser A

25 **Abstract**

26 Oral squamous cell carcinoma (OSCC) is a serious health issue worldwide. OSCC is highly

27 associated with oral candidiasis, although it is unclear whether the fungus promotes the genesis

28 and progression of OSCC or cancer facilitates the growth of the fungus. Therefore, we

29 investigated whether *Candida* could directly influence OSCC development and progression.

30 Our *in vitro* results suggest that the presence of live *C. albicans*, but not *C. parapsilosis*,

31 enhances the progression of OSCC by stimulating the production of matrix metalloproteinases,

32 oncometabolites, pro-tumor signaling routes, and overexpression of prognostic marker genes

33 associated with metastatic events. We also found that oral candidiasis triggered by *C. albicans*

34 enhanced the progression of OSCC *in vivo* through the induction of inflammation and

35 overexpression of metastatic genes and markers of epithelial-mesenchymal transition.

36 Taken together, these results suggest that *C. albicans* actively participates in the complex

37 process of OSCC progression.

38

39

40

41

42

Introduction

Oral cancer accounts for 2-4% of all cancer cases and includes a group of neoplasms that affects various regions of the oral cavity, the pharyngeal area, and salivary glands. It is estimated that more than 90% of all oral neoplasms are squamous cell carcinoma (OSCC)[1]. OSCC is the sixth most common cancer in the USA[2] and has the highest mortality rate among all oral diseases and the lowest survival rates (nearly 50%) among all cancer types. It mainly occurs in individuals over 40[1]. Regarding worldwide prevalence, a 2012 study reported that oral cancer has the highest incidence in Hungary, Pakistan and India (7 or more cases per 100,000 individuals)[3]. Risk factors of oral cancer include poor oral hygiene, tobacco, alcohol, and meat consumption[4]. OSCC and other oral tumors are typically treated by surgery, radiation, and chemotherapy. Chemotherapy and radiotherapy, when used simultaneously, provide a synergistic benefit against OSCC[5]. Currently, chemoradiotherapy is the primary treatment for OSCC leading to adverse effects such as mucositis and myelosuppression[6], which also affects the composition, quantity, and complexity of the oral microbiota[7–9].

Being the most prevalent yeasts in the oral cavity[10–12], *Candida* species, but especially *C. albicans*, are able to excessively proliferate and invade host mucosal tissues upon the disfunction or disruption of the epithelial barrier. Tissue invasion by *C. albicans* is due to the production and secretion of fungal hydrolytic enzymes, hypha formation, and contact sensing. While these phenotypic characteristics may endow *Candida* with a competitive advantage in the oral cavity, it is the host's immune competence that ultimately determines whether clearance, colonization, or disease occurs[13].

There is an association between the dysbiosis of oral yeasts and OSCC. Previous studies have revealed a higher yeast carriage and diversity in oral cancer patients compared to healthy individuals, and fungal colonisation in the oral cavity bearing OSCC is higher on the neoplastic epithelial surface compared to adjacent healthy surfaces indicating a positive association between oral yeast carriage and epithelial carcinoma[14–18]. These findings and other publications suggest that *Candida* cells may have a direct contribution to oral tumor development. One example is a case study demonstrating a rare event where persistent oral candidiasis led to the development of OSCC in an elderly patient[19]. Several other studies have confirmed the hyperplastic response of the epithelium when invaded by *Candida*. If the lesions caused by *Candida* are untreated, a minor proportion of epithelial cells may undergo dysplasia and transform into carcinoma. Thus, there is strong evidence supporting the idea that *Candida* contributes to carcinogenesis events in the oral cavity[20–24]. Additionally, patients undergoing radiotherapy for head and neck cancer are at increased risk of developing oral candidiasis as

77 fungal colonization occurs more frequently in these patients [25,26]. One study found that

78 treatment of OSCC by chemoradiotherapy resulted in oral candidiasis in 75.3% of patients[27].

79 Several other studies demonstrated a link between OSCC and *Candida* colonisation of the

80 mouth[23,28–31]. *Candida* infection in patients with cancer is usually considered to be the

81 consequence of an altered immune status because both myelosuppression and mucositis enable

82 the development of oral candidiasis[7,8,32,33].

83 To date, there is increasingly strong evidence that suggests that the development of oral

84 candidiasis in oral tumor patients enhances progression events that could result in poor

85 prognosis. Despite of this, no study has effectively investigated this phenomenon and

86 characterized the potential underlying mechanisms for *Candida* enhancing OSCC development

87 and progression. In this study, we aimed to investigate fungal-specific molecular mechanisms

88 that could facilitate and enhance cancer development or progression.

89 **Results**

90 **Heat-inactivated *Candida* and zymosan slightly increase activity related to metastasis *in***

91 ***vitro***

92 To examine the effect of the increased fungal burden on oral tumor progression, OSCC cells

93 HSC-2 and HO-1-N-1 were treated either with zymosan, heat-inactivated (HI) *C. albicans* or

94 HI-*C. parapsilosis* cells. We used zymosan - a cell wall component of *Saccharomyces*

95 *cerevisiae* – as a general fungal stimulus and HI-*Candida* treatment on the OSCC cells for

96 examining the effects of direct contacts between fungal cell wall components and OSCC cells.

97 First, a Wound Healing Assay was used to analyze the invasive capacity of OSCC cells. The

98 cellular movement of the HO-1-N-1 cell line was significantly enhanced by all applied

99 treatments compared to the untreated control (zymosan:1.445+/-0.076; HI-*C. albicans*:1.369+/-

100 0.09; HI-*C. parapsilosis*: 1.454+/-0.083). In contrast, no significant differences were observed

101 in the case of HSC-2 cells (Figure 1A). To assess host cell proliferation during fungal exposure,

102 we performed BrdU proliferation assays. The BrdU assay revealed that HI-*Candida* cells do

103 not affect tumor cell proliferation of either OSCC cell lines (Supplementary 1A).

104 A critical component of tumor cell adaptability to different environment lies in their ability to

105 remodel the extracellular matrix of the surrounding tissue, which is largely attributed to the

106 secretion of a variety of proteases (serine, cysteine, threonine, aspartic, and metalloproteinases).

107 In particular, matrix metalloproteinases (MMPs) are key enhancers of tumor dissemination[34].

108 To assess whether yeast presence affects MMP secretion and function, secreted total MMP

109 activity of the OSCC cell lines was measured. In all applied conditions significantly elevated

110 secreted MMP activity was observed in the case of HSC-2 cells compared to the untreated

111 control (zymosan: 1.516+/-0.041; HI-*C. albicans*: 1.437+/-0.06536; HI-*C. parapsilosis*:

112 1.426+/-0.057), however, the MMP activity was not altered significantly when HO-1-N-1 cells

113 were exposed to treatments (Figure 1B).

114 Metabolites generated by cancer cells influence the metastatic cascade, affecting epithelial-

115 mesenchymal transition (EMT), the survival of cancer cells in circulation, and metastatic

116 colonization at distant sites[35]. Potential changes in metabolic activity were examined by

117 analyzing the amount of glycolysis and TCA cycle intermediates, and of certain amino acids

118 (Supplementary 1C) with HPLC-HRMS. In the case of HO-1-N-1 cells, zymosan treatment

119 produced a significant change in fumaric acid (1.189+/-0.044), while HI-*C. albicans* treatment

120 altered the levels of glyceraldehyde-3P (0.580+/-0.137), aspartic acid (1.374+/-0.096), and

121 erythrose-4P (1.039+/-0.015). HI-*C. parapsilosis* treatment altered the production of

122 oxaloacetic acid (1.463+/-0.214), succinic acid (1.586+/-0.199), and glucose/fructose-6p

123 (1.317+/-0.118) (Figure 1C). For the HSC-2 cell line, zymosan treatment significantly increased

124 the production of glucose/fructose-6p (1.564+/-0.132), while HI-*C. albicans* treatment reduced

125 the concentrations of glyceraldehyde-3P (0.605+/-0.142). HI-*C. parapsilosis* treatment altered

126 levels of erythrose-4P (0.844+/-0.056), fumaric acid (0.763+/-0.065), oxaloacetic acid

127 (1.289+/-0.117), and methionine (0.855+/-0.031) (Figure 1C). Non-significant changes are

128 shown in supplementary figure 1C.

129 Taken together, HI-*Candida* and zymosan treatment had a significant effect on migration,

130 secreted MMP activity, and oncometabolite production of OSCC cells, which suggests

131 interactions between the tumor cells and the components of fungal pathogen-associated
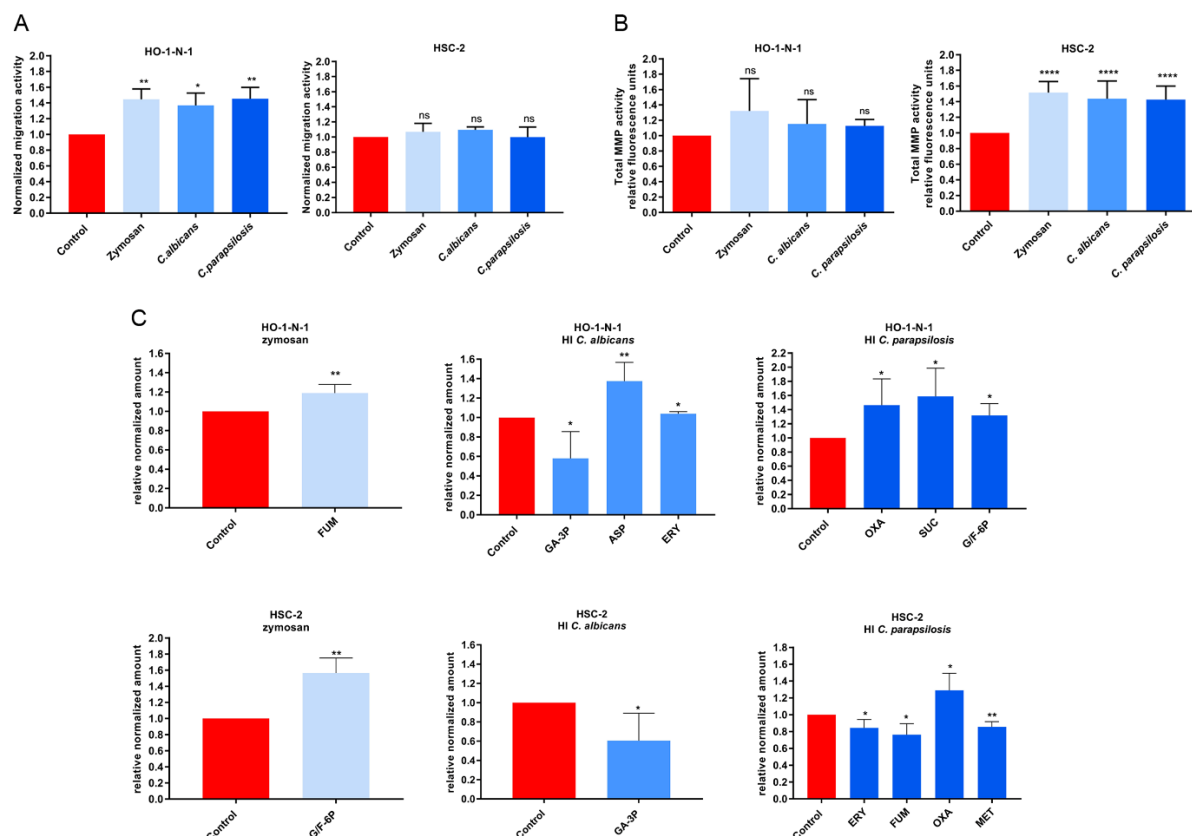
132 molecular patterns (PAMPs).

133

134 **Figure 1** Effects of HI-*Candida* and zymosan on HO-1-N-1 and HSC-2 oral squamous cell

135 carcinoma cells *in vitro*. (**A**) Normalized migration activity of OSCC cells in the presence of

136 HI-*C. albicans,* HI-*C parapsilosis* and zymosan measured by a Wound Healing Assay, n=3.

137 (**B**) Normalized total secreted matrix metalloproteinase (MMPs) activity of OSCC cells in the

138 presence of HI-*C. albicans,* HI-*C. parapsilosis* and zymosan measured by a total MMP activity

139 kit, n=4. (**C**) Normalized amounts of metabolites of OSCC cells in the presence of HI-*C.*

140 *albicans,* HI-*C. parapsilosis* and zymosan as measured by HPLC-HRMS, n=4; FUM - Fumaric

141 acid; GA-3P - Glyceraldehyde-3P; ASP - Aspartic acid; ERY - Erythrose-4P, OXA -

142 Oxaloacetic acid; SUC - Succinic acid; G/F-6P – Glucose/Fructose-6p; MET –Methionine;

143 Control: tumor cells without any treatment. Unpaired t-test; * p ≤ 0.05; ** p ≤ 0.01; ***

144 p ≤ 0.001; **** p ≤ 0.0001.

145

146 **Live *Candida* enhances detachment, MMP activity, and metabolite production of OSCC**

147 **cells *in vitro***

148 After assessing the direct interactions, we aimed to examine the indirect interplay between

149 OSCC cells and *Candida*. To accomplish this, we applied live *C. albicans* and *C. parapsilosis*

150 cells on OSCC cultures and recorded the movement of cancer cells on time-lapse video. In the

151 presence of live *C. albicans*, increased numbers of detached, single HSC-2 cells were detected

152 around the fungal cells compared to untreated control cancer cells (Figure 2A). Live *C.*

153 *parapsilosis* did not cause noticeable changes in the movement of HSC-2 cells (Supplementary

154 video 1,2,3). No change was detected in any of the fungal treatments in case of HO-1-N-1 cell

155 line (data not shown). Similar to HI-*Candida*, live *C. albicans* and *C. parapsilosis* did not cause

156 any changes in the proliferation of the OSCC cells as measured by BrdU assay (Supplementary

157 1B). Secreted total MMP activity was increased in both cancer cell lines following incubation

158 with live *C. albicans* (HSC-2: 1.918+/-0.209; HO-1-N-1: 1.918+/-0,183), but the MMP activity

159 in the presence of live *C. parapsilosis* was similar to that of the untreated control (Figure 2B).

160 Metabolic changes of OSCC cells were also measured following treatments with live *C.*

161 *albicans* and *C. parapsilosis*. No fungal metabolites could be measured after our extraction

162 method. In the case of the HSC-2 cell line, live *C. albicans* treatment led to significant changes

163 in the secretion of aspartic acid (2.67+/-0.346), glyceraldehyde-3P (0068+/-0.009), methionine

164 (0,634+/-0.063), proline (0.666+/-0.087), and succinic acid (1.975+/-0.234), while *C.*

165 *parapsilosis* treatment resulted in alterations in fumaric acid (1.199+/-0.046), glyceraldehyde-

166 3P (0.225+/-0.076), and succinic acid (1.523+/-0.101) secretion. For the HO-1-N-1 cell line, *C.*

167 *albicans* treatment significantly altered the secretion of aspartic acid (5.526+/-1.667),

168 glyceraldehyde-3P (0.543+/-0.038), glucose/fructose-6p (0.288+/-0.047), glutamine (2.616+/-

169 0.667), α-ketoglutaric acid (1.532+/-0.051), and succinic acid (9.81 +/-2.709), while *C.*

170 *parapsilosis* treatment reduced the level of aspartic acid (0.408+/-0.024) (Figure 2C).

171 The results demonstrated that live *Candida* caused prominent changes in the movement, MMP

172 activity, and metabolite production in OSCC cells compared to HI-*Candida* and zymosan
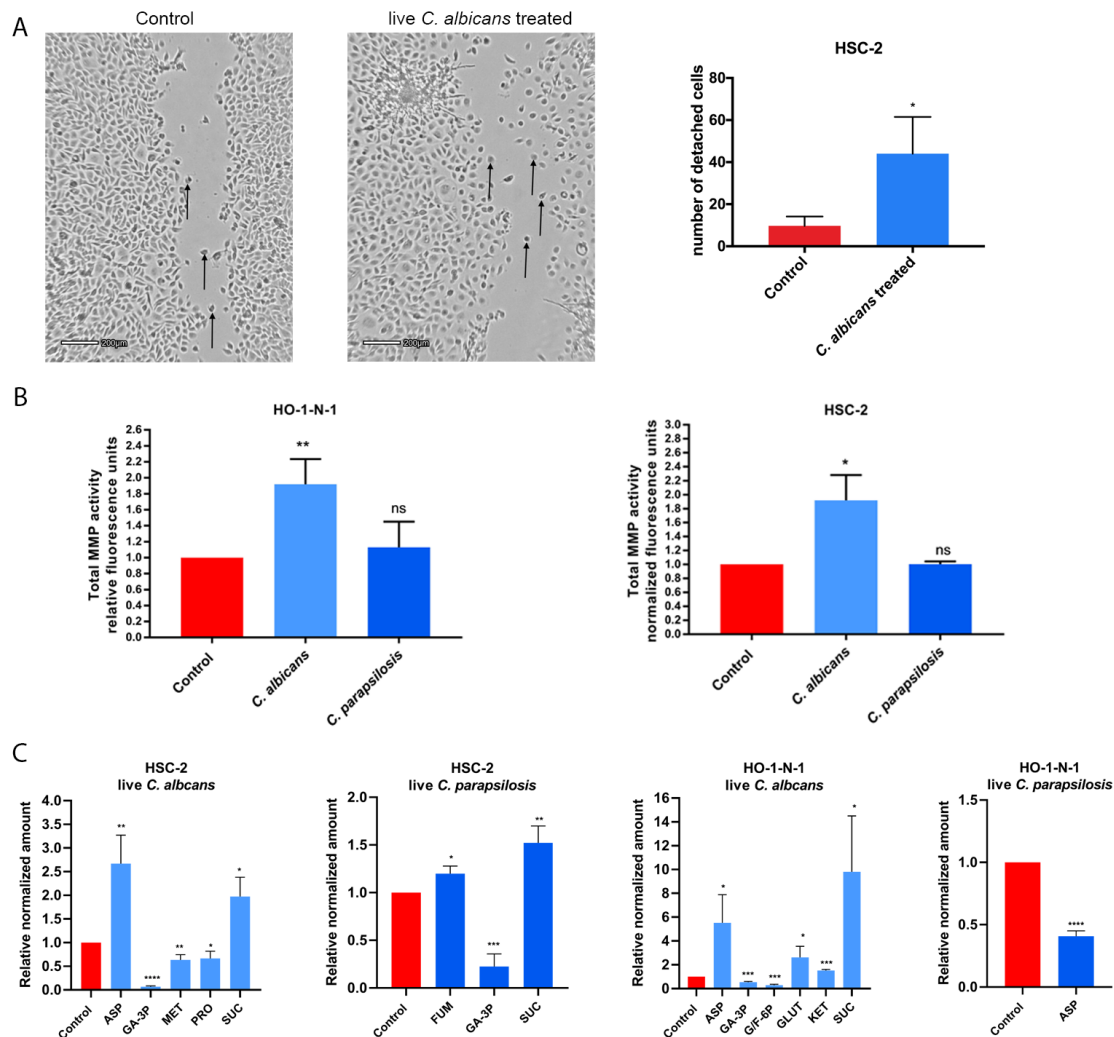
173 treatment.

Figure 2 Effects of live *Candida* on HO-1-N-1 and HSC-2 oral squamous cell carcinoma cells *in vitro.* (**A**) Pictures from time-lapse videos of cellular migration of HSC-2 cells, arrows are pointing to detached cancer cells. The left picture shows the control cells and the right shows the live *C. albicans* treated cells. The graph shows the number of detached cells, n=3. (**B**) Normalized total secreted matrix metalloproteinase activity of OSCC cells in the presence of live *C. albicans* and *C. parapsilosis* as obtained by a total MMP activity kit, n=3. (**C**) Normalized amounts of metabolites of OSCC cells in the presence of live *C. albicans* and live *C. parapsilosis* as measured by HPLC-HRMS, n=3. ASP - Aspartic acid; GA-3P - Glyceraldehyde-3P; MET –Methionine; PRO – Proline; SUC - Succinic acid; FUM - Fumaric acid; G/F-6P – Glucose/Fructose-6p; GLUT - Glutamic acid; KET - α-Ketoglutaric acid. Control: tumor cells without any treatment. Unpaired t-test; * $p \leq 0.05$; ** $p \leq 0.01$; *** $p \leq 0.001$; **** $p \leq 0.0001$

Live *C. albicans* stimulus activates genes and signaling pathways involved in the metastatic processes of OSCC

To identify and compare the molecular mechanisms of the observed cellular effects caused by each treatment, whole transcriptome analysis was performed with HSC-2 and HO-1-N-1 cells following exposure to zymosan, HI-*C. albicans*, HI-*C. parapsilosis*, live *C. albicans*, and live *C. parapsilosis*. The transcriptome analyses revealed that the highest number of statistically significant expression changes in OSCC were induced by live *C. albicans* treaments (HSC-2: n=2764; HO-1-N-1: n=137), followed by zymosan stimulus (n=19), while live *C. parapsilosis* and heat-inactivated fungal challenge did not trigger a significant response on the gene expression level in either of the OSCC cell lines. When comparing the OSCC cell lines, the evoked host response was more significant in HSC-2 (upregulated genes n=1315; downregulated genes n=1449) than in HO-1-N-1 cells (upregulated n=134; downregulated n=3) (Figure 3A) (Supplementary table2). Moreover, subsequent analyses suggest that *C. albicans* stimulus triggered significant changes in the expression of those HSC-2 genes (32 upregulated, 4 downregulated) that were previously described as marker genes of OSCC invasion (Supplementary table 4) (Figure 3B). Additional analyses provided another set of genes (21 upregulated, 3 downregulated), which overlapped with the characteristic profile of epithelial-mesenchymal transition derived from single-cell sequencing (scSeq) results from 18 patients with head and neck squamous cell carcinoma (HNSCC)[36] (Figure 3C). We found 5 genes, INHBA, MMP10, MMP1, SEMA3C, and FHL2, which were present both in the overlapping subset with the OSCC invasion marker genes and the scSeq derived gene set (Figure G). The analyses also revealed that even though the HO-1-N-1 response was modest compared to HSC-2, 13 OSCC invasion marker genes (Figure 3D) and four EMT genes (Figure E) were upregulated after live *C. albicans* stimulus. Two of these genes, SERPINE1 and INHBA, overlapped with the OSCC invasion marker genes and EMT subsets (Figure H).

KEGG pathway analysis was also performed on the data set. It revealed significant activation of several pathways in HSC-2 cells that have previously been associated with OSCC metastasis development including the Hippo signaling pathway, Focal adhesion pathway, JAK-STAT pathway, PI3K-Akt pathway, Wnt pathway, and TGFβ pathway (Figure 3F, Supplementary 2-7)[37–41]. We analyzed further the expression data in the Ingenuity pathway analysis (IPA), Qiagen's cutting-edge bioinformatical software. We employed the built-in causal analyses to investigate activation patterns of several intracellular signaling pathways based on the coherent regulation of their molecular elements. IPA analyses of the HSC-2 gene set predicted the activation of tumor-related pathways, including the tumor microenvironment pathway as well

222   as the significant activation of several prognostic features, such as metastasis, invasion,

223   angiogenesis, and proliferation of tumors based on the *C. albicans* stimulus-derived DEGs

224   (Figure 3I).

225   Interestingly, the expression of DLST and SUCLA genes in the HSC-2 cell line was slightly

226   increased in the presence of *C. albicans*, and these genes are involved in succinic acid

227   metabolism. Furthermore, ASNSD1 and GOT1 genes were also slightly upregulated and they

228   are involved in aspartic acid synthetic processes (Supplementary 9A). The identified genes and

229   signaling pathway components upregulated in HSC-2 cells in the presence of live *C. albicans*

230   were validated by qPCR (supplementary 7A-E).

231   These results support our previous findings that the presence of live *C. albicans* cells enhances

232   the metastatic features of OSCC cells, which is in contrast to that found with live *C.*

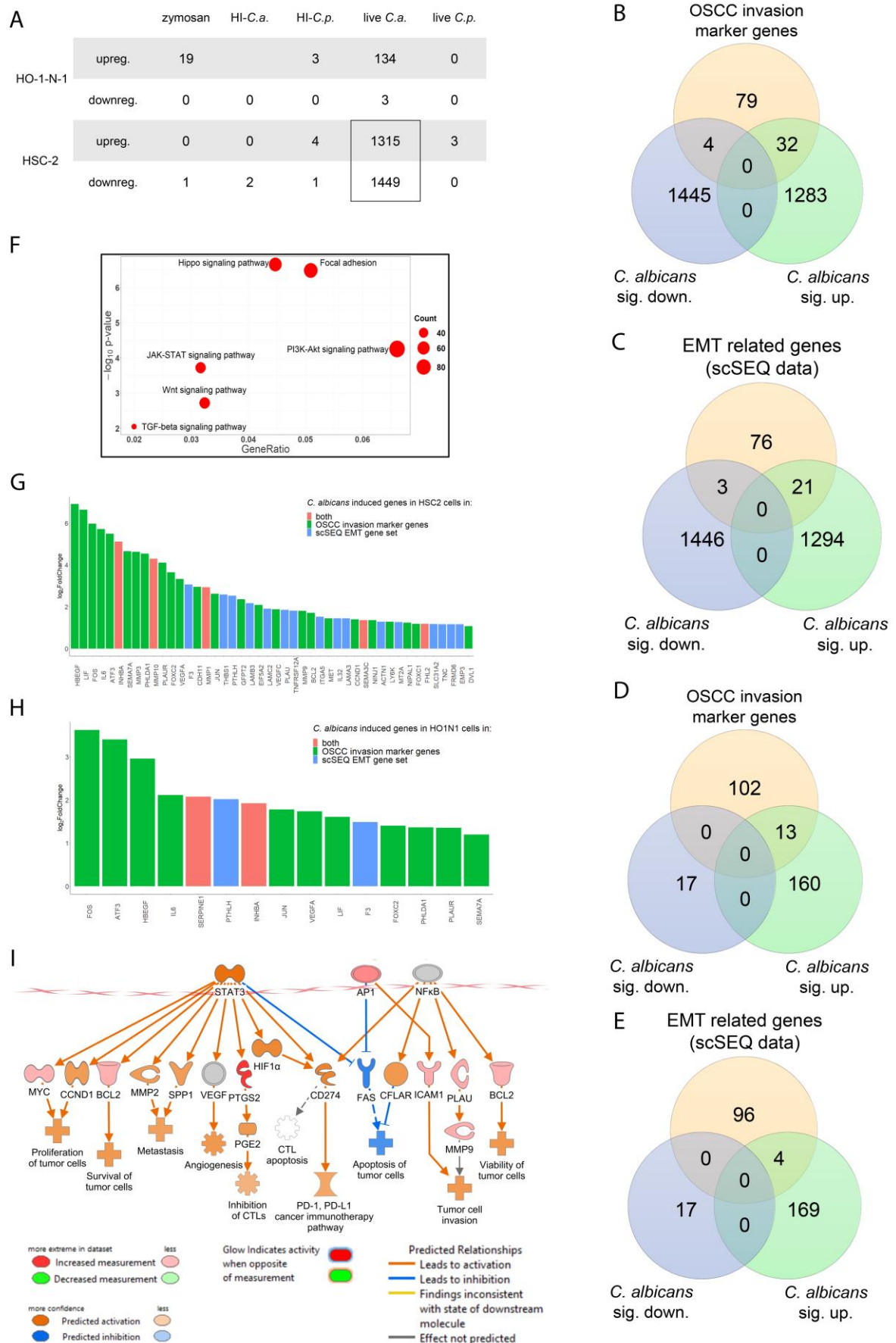233   *parapsilosis*, HI-*Candida*, or zymosan.

235 **Figure 3** *In vitro* transcriptomic analysis. *Candida albicans* activates genes and signaling
236 pathways involved in the OSCC metastatic processes. (**A**) Number of up or downregulated
237 genes of HSC-2 and HO-1-N-1 cells after different fungal treatments, n=3. (**B**) VEN diagram
238 of up or downregulated genes in HSC-2 cells in the presence of live *C. albicans* and OSCC
239 invasion marker genes found in the literature. (**C**) VEN diagram of up or downregulated genes
240 in the HSC-2 cell line in the presence of live *C. albicans* and EMT marker genes in HNSCC
241 according to a single cell sequencing study. (**D**) VEN diagram of up or downregulated genes in
242 HO-1-N-1 cells incubated with live *C. albicans* and OSCC invasion marker genes found in the
243 literature. (**E**) VEN diagram of up or downregulated genes in the HO-1-N-1 cell line in the
244 presence of live *C. albicans* and EMT marker genes in HNSCC according to a single cell
245 sequencing study. (**F**) Signaling pathways that are key regulators of the OSCC invasion
246 processes that were significantly activated in HSC-2 cells in the presence of live *C. albicans*.
247 (**G**) Graph shows log2 fold change of *C. albicans* induced genes in HSC-2 cells involved in
248 OSCC invasion according to the literature and of single-cell sequencing (scSeq) results from
249 18 patients with HNSCC. Red columns show OSCC marker genes according to the literature
250 and scSEQ data. (**H**) Graph shows log2 fold change of *C. albicans* induced genes in HO-1-N-
251 1 cells involved in OSCC invasion according to the literature and scSEQ data. Red columns
252 show OSCC marker genes according to the literature and scSEQ data. (**I**) Causal analyses of
253 the genes for which expression changed in HSC-2 cells after live *Candida albicans* treatment.
254

255 **Establishment of a novel *in vivo* mouse xenograft model of OSCC and oral candidiasis**
256 We successfully developed a novel *in vivo* mouse model of OSCC and oral candidiasis. In this
257 model we aimed to thoroughly examine the effect of oral candidiasis on OSCC progression. As
258 *C. albicans* cells are not in direct contact with HSC-2 cells in this model, only an indirect effect
259 of oral candidiasis can be examined on OSCC progression. To mimic the immunologic
260 condition of patients caused by chemoradiotherapy, cortisone acetate was administered to 6-8
261 weeks old BALB/c mice to induce an immunosuppressed condition for subsequent tumor cell
262 injection. As HSC-2 cells were more reactive to the presence of yeast cells compared to HO-1-
263 N-1, 1×10^6 cells of HSC-2 were injected in the tongues of mice to induce OSCC development.
264 According to our experiments, a fully developed tumor formed on the tongues by day 3 after
265 HSC-2 injection. After confirming the presence of a tumor, *C. albicans* saturated calcium
266 alginate swabs (placed in to 1×10^9/mL *C. albicans* suspension for 5 min) were placed under the
267 tongue of each mouse for 75 minutes on day 5 (3 days after tumor cell injection). Mice were
268 terminated on day 8 upon signs of decreased activity and weight loss (25%) to prevent

269   unnecessary suffering (*Supplementary 10C*). On the 8th day, the average tumor size was 5 mm

270   in diameter (Figure 4B). Hematoxylin-eosin (H&E) staining was performed for

271   histopathological analyses (Figure 4C). Fungal hyphae were detected on the mucosa following

272   periodic acid–Schiff (PAS) staining (Figure 4D). The oral fungal burden of mice infected with

273   *C. albicans* SC5314 was 10^5–10^6 CFU per g tissue, which is comparable with the literature of

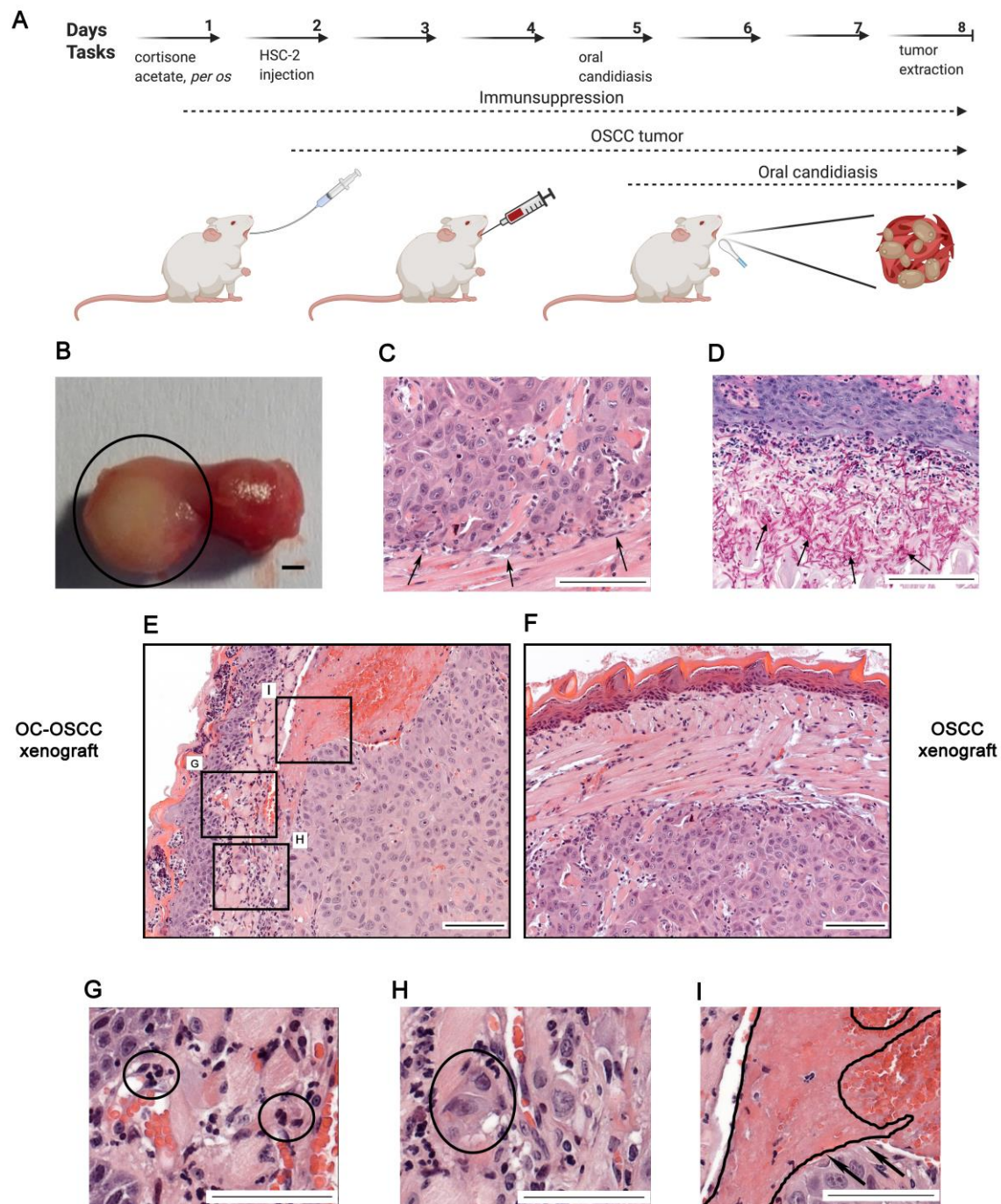274   oral candidiasis models[42].

275

276

277 **Figure 4** A new *in vivo* mouse model for the investigation of oropharyngeal candidiasis on the
278 progression of OSCC. (**A**) Schematic figure of mouse xenograft for the investigation of the
279 effect of *C. albicans* on the progression of OSCC. Immunosuppression and injection of human
280 HSC-2 OSCC cells to the tongue of mice (OSCC xenograft). OSCC xenograft and oral
281 candidiasis (OC-OSCC xenograft). The cartoon was produced by BioRender. (**B**)
282 Representative mouse tongue on the 8th day of the experiment (7 days after tumor cell injection).
283 The circle highlights the tumor. Scale bar: 1 mm. (**C**) Histopathological image of the tumor on
284 the 8th day with arrows indicating the tumor edge. Scale bar: 100 µm. (**D**) Histopathological
285 examination of the tumor on the 8th day (7 days after tumor injection and 3 days post-infection)
286 with black arrows indicating the fungal hyphae in the mucosa. Scale bar: 100 µm (**E**)
287 Histopathological picture about the tumor on the 8th day after HSC-2 injection and oral
288 candidiasis (OC-OSCC xenograft, n=4 derived from four different experiments) Scale bar: 100
289 µm. (**F**) Histopathological picture about the tongue on the 8th day after HSC-2 injection (OSCC
290 xenograft, n=4 derived from four different experiments). Scale bar: 100 µm. (**G**) Infiltrating
291 immune cells in OC-OSCC xenograft samples indicating *C. albicans* caused inflammation.
292 Scale bar: 100 µm. (**H**) Detached budding tumor cells in OC-OSCC xenograft samples
293 indicating epithelial to mesenchymal transition. Scale bar: 100 µm (**I**) Thrombosis in OC-OSCC
294 xenograft samples. Scale bars: 100 µm.

295

296 **Oral candidiasis enhances the progression of OSCC *in vivo***
297 For investigating the effect of increased yeast burden on OSCC progression two animal groups
298 were compared: one group received only cortisone acetate and HSC-2 human tumor cells
299 (OSCC xenograft), while another group of animals received cortisone acetate, HSC-2 cells and
300 *C. albicans* treatment for the development of oral candidiasis (OC-OSCC xenograft). Each
301 group (OSCC and OC-OSCC xenograft) contained 4-4 animals derived from four different
302 experiments. Histopathological samples of *Candida*-colonized and *Candida*-free tumors were
303 analysed and scored manually in a blinded manner by a pathologist after H&E staining for the
304 identification of inflammation, necrosis, infiltrating or pushing tumor edge, epithelial-
305 mesenchymal transition (EMT), invasion markers, and signs and symptoms of thrombosis and
306 peritumoral inflammation (Supplementary 10A). EMT and budding of tumor cells were more
307 frequent in 2 samples out of 4 in the case of oral candidiasis compared to control tumors.
308 Interestingly, thrombosis was also detected in 3 OC-OSCC xenograft samples. Only one sample
309 showed thrombosis in OSCC xenograft.

310   Infiltrating immune cells were detected within the OC-OSCC xenograft samples, indicating *C.*

311   *albicans*-induced inflammatory responses (*Figure 4G*). Images indicative of epithelial-

312   mesenchymal transition were also identified, as represented by the increased number of

313   detached individual tumor cells (Figure 4H). Interestingly, significant thrombosis was noted on

314   the histopathological samples derived from OC-OSCC xenograft mice (*Figure 4I*).

315   Taken together, histopathological scoring suggests the presence of oral candidiasis-driven

316   OSCC progression events.

317

318   **Oral candidiasis increases p63 and vimentin expression and decreases E-cadherin**

319   **expression in OSCC histopathological specimens**

320   p63 expression is a reliable indicator in histological grading and is an early marker of poor

321   OSCC prognosis. When comparing the p63 histopathological staining of the OSCC xenograft

322   and OS-OSCC xenograft samples, analysis of OC-OSCC xenograft samples showed that *C.*

323   *albicans* treatment increased p63 expression and localisation to the nucleus compared to the

324   uninfected tissues (Figure 5A). Next, we analyzed the expression of EMT markers by

325   performing E-cadherin and vimentin staining. Robust expression of E-cadherin was observed

326   in the cell membrane of the OSCC xenograft tumors whereas OC-OSCC xenograft samples

327   demonstrated attenuated E-cadherin expression (Figure 5B). Vimentin was detected in the

328   cytoplasm of only a few cells in OSCC xenograft sections, but many vimentin-positive cells

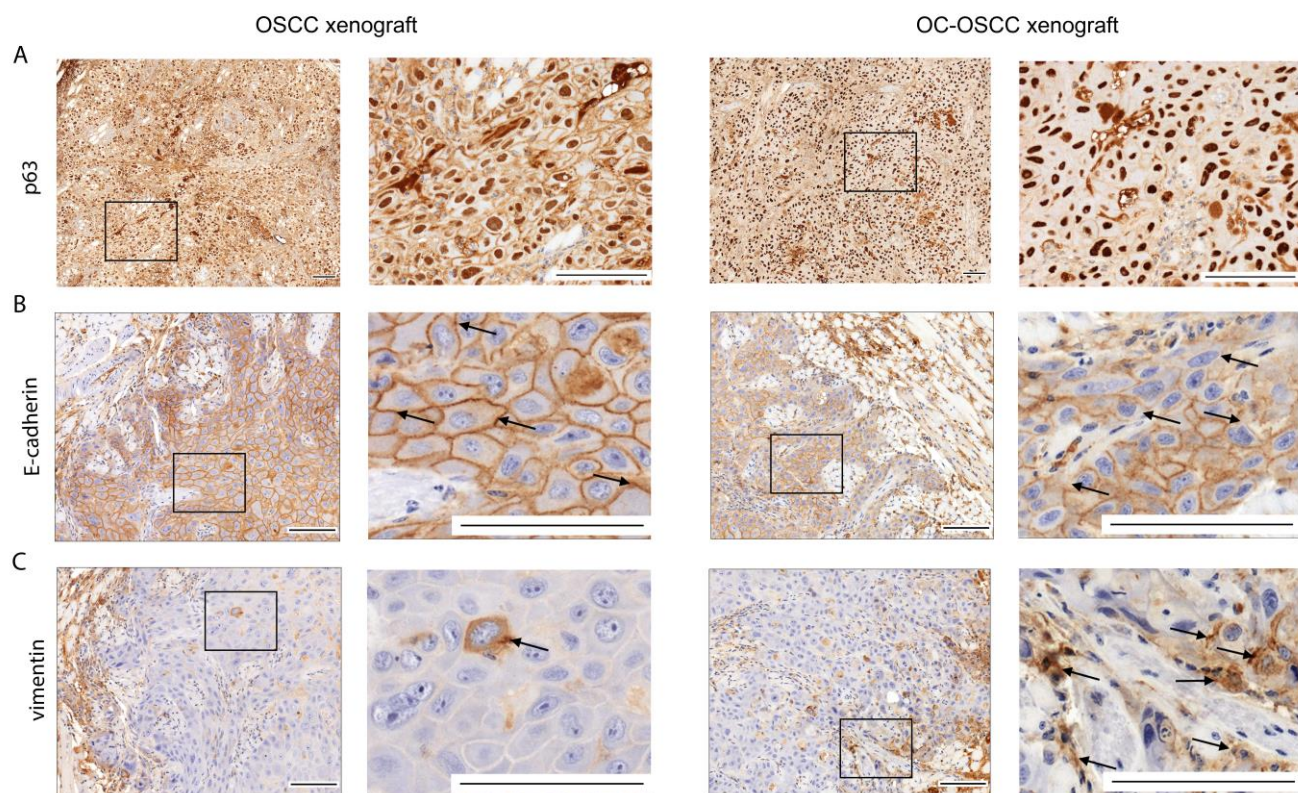329   were observed in the OC-OSCC xenograft samples (Figure 5C).

Figure 5 Histopathological staining of OSCC and OC-OSCC xenograft tumor samples: (**A**) p63 staining, (**B**) E-cadherin staining, and (**C**) Vimentin staining. Scale bars: 100 μm. n=4/animal group, derived from four different experiments.

Oral candidiasis enhances the expression of genes involved in OSCC progression *in vivo*

To analyze the molecular mechanisms behind the histopathological results, transcriptome analysis of OC-OSCC xenograft tumor samples was performed and data were compared to that of OSCC xenograft tumors (Figure 6A). Obtained data analyses showed that oral candidiasis in OSCC xenografts altered the expression of 229 genes (144 upregulated and 85 downregulated) (Supplementary table 2). Among these, 5 genes (MMP10, MMP1, SERPINB4, and CRABP2 upregulated; MMP7 downregulated) are predicted to be involved in OSCC invasion processes (Figure 6B), while 3 genes (MMP10, MMP1, and COL5A2 upregulated) are associated with epithelial-mesenchymal transition regulation (Figure 6C). Notably, MMP10 and MMP1 were present in both subsets (Figure 6D) and were also upregulated in both our *in vitro* and *in vivo* models (Figure 6E).

347

348
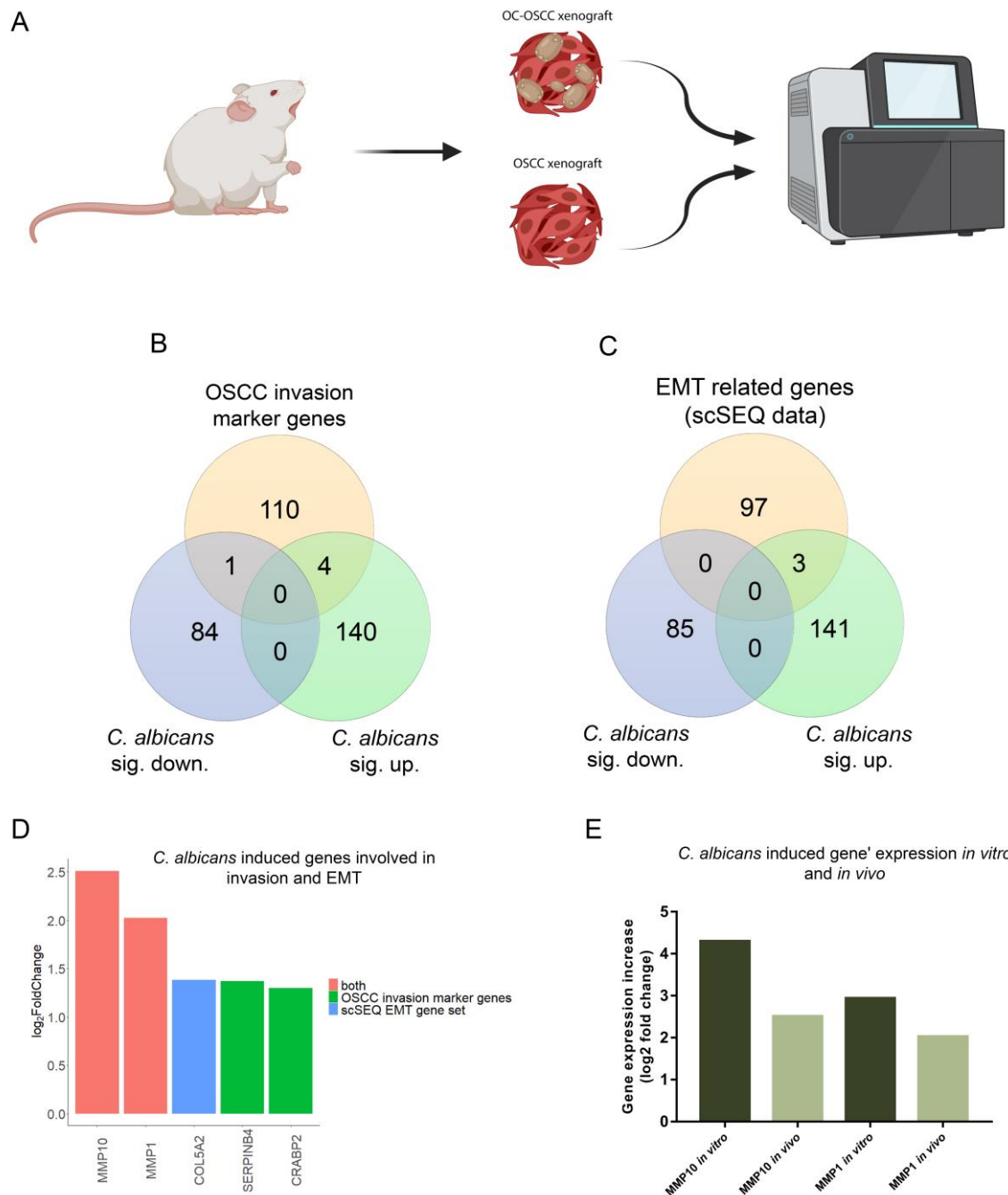
349 **Figure 6** Transcriptomic analysis of *in vivo* tumor samples followed by oral candidiasis. (**A**)

350 Schematic figure of mRNA sequencing of OSCC xenograft and OC-OSCC xenograft tumor

351 samples. The cartoon was produced by BioRender. (**B**) VEN diagram of up or downregulated

352 genes in HSC-2 cells in the presence of live *C. albicans* and OSCC invasion marker genes

353 described in the literature. (**C**) VEN diagram of up or downregulated genes in HSC-2 cell line

354   in the presence of live *C. albicans* and EMT marker genes in HNSCC according to a single cell

355   sequencing study. (**D**) Graph shows log2 fold change of *C. albicans* induced genes in HSC-2

356   cells involved in OSCC invasion according to the literature and single-cell sequencing data.

357   Red columns show OSCC marker genes according to both the literature and single-cell

358   sequencing (scSeq) results from 18 patients with HNSCC (**E**) Tumor invasion genes showing

359   upregulated expression both *in vitro* and *in vivo*.

360   n= 4/animal group, derived from four different experiments.

361

Discussion

363   OSCC is highly associated with the presence of oral candidiasis. However, the details of the

364   cause versus causative relationship are not understood[25–31] . Our previous study showed that the

365   diversity of the oral fungal microflora of OSCC patients is remarkably different from healthy

366   individuals: the fungal burden and diversity of yeasts was significantly higher in patients with

367   oral tumors compared to the oral cavity of healthy individuals. Furthermore, fungal colonisation

368   in the oral cavity in patients with OSCC is higher on the neoplastic epithelial surface compared

369   to healthy surfaces, which indicates a positive association between oral yeast carriage and

370   epithelial carcinoma [14]. *Candida* might induce carcinogenesis by the production of carcinogenic

371   compounds, for example, nitrosamines[43]. These carcinogens bind to bases, phosphate residues,

372   and/or hydrogen bonding sites of DNA that could interfere with DNA replication. Induced point

373   mutations might activate oncogenes and initiate the development of oral cancer. Accumulation

374   of acetaldehyde, a by-product of ethanol metabolism that is also considered to be carcinogenic,

375   and the induction of proinflammatory cytokines could also contribute to oral cancer

376   development[44], both of which are triggered by the presence of *Candida* cells.

377   *C. albicans* and *C. parapsilosis* both are common commensals of the oral cavity [45]. Both are

378   also opportunistic human pathogenic fungi, although *C. albicans* is more frequently associated

379   with oral candidiasis compared to *C. parapsilosis*[46]. *C. albicans* is truly polymorphic, due to its

380   ability to form hyphae and/or pseudohypha[47]. Concerning *C. parapsilosis*, this species does not

381   produce true hyphae but can generate pseudohyphae that are characteristically large and

382   curved[48]. Hypha formation is critical for host cell damage and immune activation, which are

383   both driven by the secretion of Candidalysin, a peptide toxin. Candidalysin damages epithelial

384   membranes and activates danger response pathways, which results in immune activation and

385   the secretion of cytokines and chemokines[49].

386   In this study, we aimed to examine the potential effects of an increased fungal burden on the

387   progression of oral squamous cell carcinoma. During the experiments, HI-*Candida*, zymosan

388 and live *Candida* cells were applied to two OSCC cell lines, HSC-2 and HO-1-N-1. To examine

389 the potential pro-tumor effect of direct cell-cell interactions, first host cell proliferation and

390 migration were assessed. A previous study showed that Gram-negative bacteria facilitated

391 proliferation and invasion activity of non-small cell lung cancer cells[50]. During our experiments

392 we could not detect any significant changes in host cell proliferation after the applied stimuli;

393 however, the migration activity of the HO-1-N-1 cell line significantly increased after HI-fungal

394 and zymosan treatment. Live cell imaging revealed separately migrating HSC-2 tumor cells

395 from the edges of the disrupted regions of the tumor monolayer after exposure to live *C.*

396 *albicans* cells. As several of the segregated cells appeared distinctly from the plate-attached

397 hyphae of *C. albicans* cells, we assume that an indirect interaction could also take place between

398 tumor and yeast cells possibly through secreted molecules or extracellular vesicles[51]. This may

399 play a role in tumor progression by the enhancement of invasion. No such phenomenon was

400 observed in the presence of live *C. parapsilosis* cells.

401 Matrix metalloproteinases (MMPs) are essential to the tumor metastasis processes, as their

402 secretion degrades components of the extracellular matrix elements, facilitating the migration

403 of individual malignantly transformed cells[52]. Notably, as a result of HI fungal challenge and

404 zymosan treatment, we detected a slight increase in secreted MMP activity. Additionally, live

405 *C. albicans* treatment resulted in a marked increase in MMPs activity, supporting the hypothesis

406 that *C. albicans* can increase tumor invasion by the activation of MMPs. Live *C. parapsilosis*

407 treatment did not trigger an increase in MMP concentrations. Our transcriptomic results also

408 support this finding as *C. albicans* induced the expression of several MMP genes in the HSC-2

409 cell line.

410 Metastatic tumor cells have unique metabolic profiles[53]. For this reason, we examined the

411 concentrations of glycolysis, TCA cycle intermediated and some amino acids with HPLC-

412 HRMS with and without exposure to *Candida* or zymosan. Metabolic analysis revealed that

413 HI-*Candida* and zymosan treatments result in only a slight and inconsistent alteration in the

414 production of a few metabolites. In contrast, live *C. albicans* cells increased the amount of

415 aspartic acid and succinic acid and decreased the amount of glyceraldehyde-3P in both OSCC

416 cell lines. Transcriptomic and qPCR results also support these findings. Gene expression of

417 GOT1, DLST and SUCLA2, involved in aspartic and succinic acid synthesis, was significantly

418 increased.   Interestingly, the amount of glyceraldehyde-3P also decreased in both cell lines

419 after HI-*C. albicans* treatment compared to the untreated control. Succinic and aspartic acid

420 play a role in tumor invasion. Succinate may function as a driver of tumorigenesis through

421 multiple mechanisms. The accumulated succinate itself can inhibit prolyl hydroxylase. This

422   enzyme is responsible for hydroxylation of HIF1α causing its degradation. Therefore, succinate

423   accumulation through inhibition of prolyl hydroxylase causes HIF1α stabilization and its

424   translocation to the nucleus, which might enhance angiogenesis, resistance against apoptosis,

425   and the activation of genes involved in tumor invasion[54]. According to another study, the

426   secreted tumor-derived succinate belongs to a novel class of cancer progression factors,

427   inhibiting tumor-associated macrophage polarization and promoting tumorigenic signaling

428   through PI3K/AKT and HIF-1α[55]. Another study showed that aspartate is a limiting metabolite

429   for cancer cell proliferation under hypoxia and in tumors, such that aspartate might be a limiting

430   metabolite for tumor growth[56]. This suggests that the *C. albicans* induced aspartic acid increase

431   may facilitate OSCC progression. We assume that the reduced GA-3P levels could be the result

432   of increased glyceraldehyde-3-phosphate dehydrogenase (GAPDH) activity. GAPDH catalyzes

433   the redox reaction in the glycolytic pathway by converting GA-3P to 1,3-bisphosphoglycerate

434   with a reduction of NAD^+ to NADH. GAPDH promotes cancer growth and metastasis through

435   upregulation of SNAIL expression[57]. Increased succinic and aspartic acid, and decreased GA-

436   3P suggest that the presence of live *C. albicans* might enhance OSCC progression by altering

437   complex metabolic processes in tumor cells.

438   Transcriptome analysis results also supported our *in vitro* findings as the presence of live *C.*

439   *albicans* cells alters the metastatic features of OSCC cells, while HI-*Candida* and zymosan

440   stimuli had a mild effect. Comparing the two cell lines, HSC-2 showed more prominent

441   responses to live *C. albicans* treatment in terms of the activation of genes and pathways than

442   HO-1-N-1 cells. In both cell lines, we identified several *C. albicans*-induced genes that are

443   involved in OSCC invasion and metastasis regulation (Supplementary table4). Among the

444   overlapping genes, there were 14 *C. albicans*-induced genes (ATF3, F3, FOS, FOXC2,

445   HBEGF, IL6, INHBA, JUN, LIF, PHLDA1, PLAUR, PTHLH, SEMA7A, and VEGFA) whose

446   expression increased in both cell lines.

447   The obtained transcriptomic data support our *in vitro* findings on total MMP activity and

448   oncometabolite secretion. We detected a significant increase in MMP1, MMP10, MMP3, and

449   MMP9 expression, and a slight increase in the expression of ASNSD1, GOT1, DLST,

450   SUCLA2, all of which are involved in aspartic and succinic acid metabolism. All obtained

451   transcriptomics data were further validated by qPCR.

452   To examine whether live *C. albicans* enhances invasion and metastatic activity of OSCC *in*

453   *vivo*, we developed a novel *in vivo* mouse model of OSCC and oral candidiasis. Human HSC-

454   2 OSCC cells were injected into the tongue of the immunosuppressed BALB/c mice. After oral

455   tumor development, xenograft mice were infected with *C. albicans* to induce oral candidiasis

456   development. During the subsequent experiments, yeast-free tumor samples were compared to

457   *C. albicans*-colonized tumors derived from the xenograft groups. In the OC-OSCC tongues,

458   infiltrating immune cells were observed on the mucosa, which was further characterized as

459   having severe inflammation caused by *C. albicans*. Signs of inflammation could also be

460   observed in the tumor tissue. Inflammatory cells promote the development, advancement, and

461   metastasis of cancer by producing tumor-promoting cytokines. Furthermore, inflammation can

462   alter the tumor microenvironment by inducing growth, survival, proangiogenic factors, and

463   reactive oxygen species. It can also modify the extracellular matrix, thereby promoting

464   angiogenesis, invasion, and metastasis[58]. EMT plays a vital role in invasion and metastasis of

465   cancer cells[59]. Thrombosis was also detected in 3 OC-OSCC xenograft samples. The

466   relationship between thrombosis and tumor invasion is well established, but the details of the

467   exact pathological processes are not yet known. Although the details of the process are

468   unknown, thrombosis promotes metastasis[60]. To further evaluate the metastasis enhancing

469   effect of *C. albicans*, we performed p63 staining on histopathological samples. p63 is the

470   protein encoded by the *TP63* gene, a *TP53* gene homolog, known for its key role in cell cycle

471   regulation and in tumor differentiation. Its overexpression is associated with a poor prognosis

472   of head and neck squamous cell carcinoma[61]. p63 has two different promoter domains that

473   produce TAp63, which includes an NH_2-terminal transactivation domain, and ΔNp63, which

474   lacks an NH_2-terminal domain. ΔNp63 enhances EMT events during tumor progression by

475   competing with TAp63 and p53 for binding sites[61,62]. In OC-OSCC xenograft samples, p63

476   expression and localisation to the nucleus was higher compared to the OSCC xenograft samples.

477   We validated this by qPCR in HSC-2 cells in which the ΔNp63 (lacks N-terminal domain)

478   transcript variant can be found (Supplementary 11). In order to further examine EMT

479   progression in OC-OSCC xenograft samples, we performed vimentin and E-cadherin staining.

480   Vimentin is a cytoskeletal protein that is expressed in mesenchymal cells (fibroblast,

481   endothelial cell, lymphocytes), but not in healthy epithelial cells and its upregulation in tumors

482   is linked with lymph node metastasis[63]. Increased vimentin expression is associated with poor

483   prognosis in OSCC[64–66]. In histopathological sections OC-OSCC samples, we detected more

484   vimentin-positive cells than in OSCC samples. E-cadherin, a 120 kDa transmembrane adhesion

485   receptor, apart from being responsible for cell-cell adhesion in the epithelium, plays an

486   important role in determining cell polarity and is also involved in several signal transduction

487   pathways (e.g., induction of apoptosis, growth factor receptor activation)[67,68]. A previous study

488   showed that the reduced expression of E-cadherin is a reliable indicator of increased

489   invasiveness of OSCCs[69]. OSCC tumor samples showed E-cadherin membrane positivity, in

490   contrast to this OC-OSCC samples showed reduced E-cadherin membrane positivity. Increased

491   p63 and vimentin expression and decreased E-cadherin expression in the isolated *Candida*

492   colonized tumors altogether indicate a poor prognosis for oral candidiasis-associated OSCC.

493   Importantly, subsequent transcriptome analysis results of the *in vivo* OC-OSCC samples

494   revealed that the presence of *C. albicans* cells induced a similar effect under these experimental

495   arrangements as in the *in vitro* setting. The expression of MMP1, MMP10, COL5A2,

496   SERPINB4, and CRABP2 was increased under both conditions, confirming the OSCC

497   progression enhancing effect of live *C. albicans* cells.

498   Oral candidiasis in OSCC patients frequently develops and is thought to exacerbate poor

499   prognosis. Prior to our work, no studies rigorously investigated this phenomenon. In this study

500   we have shown that oral candidiasis indeed aids tumor progression by exacerbating the

501   expression of tumor invasion and metastasis-associated prognostic markers. Given that oral

502   candidiasis frequently develops in oral tumor patients, as the consequence of

503   chemoradiotherapy, it therefore increases the risk for tumor invasion and metastasis. Thus,

504   applying antifungal treatment simultaneously with chemotherapy might be recommended in

505   this patient cohort. Although the efficacy of such a combined treatment option still needs to be

506   addressed, the hereby gained data provide a strong basic understanding of the nature of yeast-

507   tumor interactions which could contribute to the initiation of subsequent translational

508   investigations.

509

510   **Materials and methods**

511   **Ethics Statement**

512   The study conformed to EU Directive 2010/63/EU and was approved by the regional Station

513   for Animal Health and Food Control (Csongrád-Csanád, Hungary) under project license

514   XXIX./4061/2020.

515

516   **Cell lines and maintenance**

517   Two human oral squamous cell carcinoma (OSCC) cell lines were used. HSC-2 (JCRB0622)

518   cells were cultured in EMEM (Eagle's Minimum Essential Medium; Lonza), while HO-1-N-1

519   (JCRB0831) cells were cultured in DMEM/F-12 (Dulbecco's Modified Eagle Medium:F12;

520   Lonza) medium, both containing 10% heat-inactivated (56°C, 30 min) fetal bovine serum (FBS)

521   (EuroClone) supplemented with 4 mM glutamine, 100 U/mL penicillin and 100 mg/mL

522   streptomycin. Cells were maintained at 37°C in the presence of 5% CO_2.

523

Wound Healing Assay to assess cellular migration

HSC-2 and HO-1-N-1 cells were seeded at 3×10^5 cells/well in 6-well plates per well. Cells were allowed to grow until 100% confluency. Scratches were made in across the confluent cells using a P100 pipette tip. Zymosan (10 µg/mL working concentration) or heat-killed (HI) (65°C, 2 h) or live *C. albicans* SC5314 (SZMC 1523) or *C. parapsilosis* CLIB 214 (SZMC 1560) were used as fungal treatments. In the case of HI-*Candida*, the multiplicity of infection (MOI) was 1:10 (tumor cell : yeast). Images were taken at time point 0 h (immediately after treatment) and 24 h. Cell migration speed was analyzed using imageJ software.

The rapid hyphae formation of live *C. albicans* cells did not allow a comprehensive analysis of the extent of cancer cell movement after 24 h. Thus, a 24 h time-lapse (CytoSMART) video was analysed to examine the extent of tumor cell migration. For this, experiment, 1×10^5 tumor cells were seeded in to 24-well plates using 500 µm culture inserts and grown until full confluency. On the following day, the insert was removed and live *Candida* (*C. albicans* MOI 1:400; *C. parapsilosis* MOI 1:4) were added and imaged by time-lapse video with CytoSMART Lux2.

BrdU incorporation assay

Cell proliferation activity was measured by BrdU incorporation assay using a Cell Proliferation ELISA kit (Sigma-Aldrich). The wells of 96-well plates were seeded with 5000 HSC-2 or HO-1-N-1 cells. The following day, cells were treated with zymosan (10 µg/mL), HI-*Candida* (MOI 1:10), live *C. albicans* (MOI 1:400) or *C. parapsilosis* (MOI 1:4) for 24h, and then BrdU assay was performed according to the manufacturer's instructions. The experiment was performed in media supplemented with 1% FBS, 4 mM glutamine, 100 U/mL penicillin and 100 mg/mL streptomycin.

Sample preparation for metabolic analysis

For metabolomic analyses, 1.5×10^5 HSC-2 and HO-1-N-1 tumor cells were seeded per well in 6-well plates. On the following day, cells were treated with zymosan (10 µg/mL) or HI-*Candida* (MOI 1:10) for 24h. After removal of medium, tumor cells were washed with PBS and extracted by addition of 500 µl ice cold mixture of HPLC grade methanol:water (4:6 v/v), and the remaining debris was removed by scraping (20 mm blade width). Cell lysates was transferred to microcentrifuge tubes and sonicated for 5 min at 23kHz in an ice water bath. Sonicated samples were mixed for 15 sec and centrifuged at 13.800xg for 10 min at 4°C. The supernatants were transferred to HPLC vials and stored at -80°C.

558   Due to the rapid hyphal formation of the live *C. albicans*, for the live yeast conditions, HSC-2
559   and HO-1-N-1 cells were seeded in 6-well plates (1.5×10^5/well) in 5 technical replicates. After
560   4 h, the completely attached cancer cells were treated with live *C. albicans* (MOI 1:400) or *C.*
561   *parapsilosis* (MOI 1:4) for 24 h. After removal of culture media, the cells were washed
562   immediatelly 1x in 37°C Ringer's solution, than 2x in 37°C HPLC grade distilled water.
563   Metabolite extraction was performed by incubation of the samples in 500 μl HPLC grade
564   distilled water for 15 min causing osmotic shock for the tumor cells, while the fungal cell wall
565   remained intact according to the literature[70] and based on our measurement of the supernatants
566   collected from the *Candida* cells incubated in distilled water for 15 min, where no any
567   metabolites were detected. Samples were then centrifuged at 13.800xg for 10min at 4°C and
568   the supernatants were transferred to HPLC vials and stored at -80°C.

569

570   **High performance liquid chromatography coupled with high resolution mass**
571   **spectrometry (HPLC-HRMS) analysis of metabolites**

572   The amount of the intermediaries of glycolysis, TCA cycle and amino acids were determined
573   by HPLC-HRMS. The measurements were carried out on a Dionex UltiMate 3000 (Thermo
574   Scientific) HPLC system coupled to a Q Exactive Plus (Thermo Scientific) HRMS, where the
575   eluent A was water and eluent B was methanol supplemented both of them with 0.1% acetic
576   acid. The applied gradient program was the following on a Synergi Polar-RP (Phenomenex)
577   250x3 mm, 4 μm column for the eluent B: 0 min - 20%, 2 min – 20%, 4 min – 30%, 6 min –
578   95%, 9 min - 95%, 9.5 min - 20% and 15 min 20%. The flow rate and the injection volume
579   were 0.2 mL/min and 5 μL, respectively, while the column and the autosampler were
580   thermostated at 30°C and 4°C, respectively. The HRMS was operated with heated electrospray
581   ionization (HESI) source in parallel reaction monitoring (PRM) acquisition mode with polarity
582   switching. During the measurements, the spray voltages were 4 kV and 3 kV in positive- and
583   negative ionization modes, respectively. The sheath gas was 30, the aux gas was 15 arbitrary
584   unit, the aux gas heater temperature was 250°C and the ion transfer capillary temperature was
585   250°C in both ionization modes. The isolation window was 0.4 *m/z* and the resolution was
586   35000 (at *m/z*=200). The precursor mass, fragment ion mass, polarity, retention time and
587   fragmentation energy and the lower limit of determination (LLOQ) of the examined metabolites
588   are detailed in (Supplementary table 1). For quantitative determinations, seven level calibration
589   curves were used in the case of each metabolite, in the range of 5-5000 ng/mL. The calibration
590   standard solutions were created in MeOH:H2O 4:6 solution with equal amount internal standard
591   (250 ng/mL) compared with the tumor cell extracts. For the live *Candida* treatment conditions,

592   calibration standard solutions were created in HPLC grade distilled water. Finally, the

593   concentration values were compared with the control samples.

594

Matrix metalloproteinases (MMP) enzymatic activity

596   MMP activity was measured using the MMP activity Assay Kit (Abcam, ab112146), following

597   the manufacturer's instructions. For the experiments $3x10^5$ cells were seeded into T25 flasks.

598   On the following day, cells were treated with zymosan (10 µg/mL), HI-*Candida* (MOI 1:10),

599   live*C. albicans* (MOI 1:400) or *C. parapsilosis* (MOI 1:4) for 24 h in 4 mL serum-free medium.

600   Next, the media was collected and centrifuged for 5 min, 3000xg and 4 mL of the supernatant

601   was concentrated to appoximately 200 µL by centrifugation for 25 min at 7500xg using a

602   centrifugal filter (Amicon Ultra-4, UFC800324). The concentrated samples were adjusted to

603   same volume. Activities of MMPs was measured with fluorescence plate reader at Ex/Em =

604   490/525 nm.

605

RNA extraction for sequencing *in vitro* samples

607   For RNA extraction, $1x10^5$ HSC-2 and HO-1-N-1 cells were seeded into 24-well plates with

608   three technical replicates. After 12 h, the tumor cells were treated with zymosan (10 µg/mL),

609   HI-*C. albicans* (MOI 1:10), HI-*C. parapsilosis* (MOI 1:10), live *C. albicans* (MOI 1:25) or live

610   *C. parapsilosis* (MOI 1:4) for 12 h. After fungal treatment, mRNA was purified using the

611   RNeasy Plus Mini Kit (Qiagen) according to the manufacturer's protocol. RNA quality and

612   quantity was analyzed by Bioanalyzer Instrument (Agilent). Library preparation and

613   sequencing on a NovaSeq S4 platform was performed by Novogene.

614

RNA Sequencing

616   The preparation of mRNA sequencing library was done by external specialists at Novogene.

617   Briefly, sequencing libraries were generated using NEBNext® Ultra TM RNA Library Prep Kit

618   for Illumina® (NEB, USA) following the manufacturer's recommendations. For the

619   purification of mRNA samples, poly-T oligo-attached magnetic beads were used, then size

620   selected cDNAs were synthesized with Ampure XP system (Beckman Coulter, Beverly, USA).

621

Transcriptome analysis

623   RNA sequence files were also processed by Novogene; however, the analyses of *in vivo*

624   samples were repeated using our in-house protocol. According to the Novogene analysis

625   pipeline, raw sequence reads processed for quality via fastp, reads with adaptor contamination,

626 high precentage (N > 10%) of misread or uncertan bases and low quality (phred < 20) were

627 filtered out. Clean read files were aligned to the reference genome index (GRCh38) using

628 'HISAT2', with the parameters --dta –phred33. Read counts of known and novel genes were

629 quantified as reads per kilobase of exon model per Million mapped reads (RPKM) via

630 'Featurecounts'. This step in the case of the *in vivo* samples was interchanged with the

631 'GenomicAlignments' package resulting in counts. Differential gene expression in logarithmic

632 fold change (LFC) was then concluded using the 'DeSeq2' tool. Objects with read counts lower,

633 than 1 part per million (ppm) were filtered out. In the experimentally derived gene list,

634 differentially expressed genes (DEGs) were assigned above the absolute value of LFC > 1 and

635 the adjusted p-value < 0.05. False discovery rate was minimized using the Benjamini and

636 Hochberg's approach.

637

Causal analyses

639 We employed causal analyses methods included in Ingenuity Pathway Analysis (IPA),

640 including (i) Upstream regulatory analysis (URA) to identify probable upstream regulators and

641 (ii) Causal network analysis (CNA) to observe connections between these above mentioned

642 regulatory molecules. A priori an expression core analysis was run on the experimentally

643 derived gene set to obtain a suitable input for these analysis, and predictions with p-value of

644 overlap < 0.05 and z-score different than 0 were considered significant hits. We further

645 specified that only experimentally proven or strongly predicted intermolecular relationships

646 should be considered.

647

cDNA synthesis and reverse transcription-PCR for validation sequencing data

649 A total of 1 µg RNA was used for cDNA synthesis using a RevertAid First Strand cDNA

650 synthesis kit (Thermo Scientific) according to the manufacturer's instructions. Real-time PCR

651 was carried out in a final volume of 20 µl using Maxima SYBR green/fluorescein qPCR (2x)

652 Master Mix (Thermo Scientific). The reaction was performed in a C1000 thermal cycler (Bio-

653 Rad) using the following reaction conditions: 95°C for 3 min, 95°C for 10 s, 60°C for 30 s, and

654 65°C for 5 s for 50 cycles. Fold change in mRNA expression was calculated by the threshold

655 cycle ($\Delta\Delta$CT) method (real-time PCR applications guide; Bio-Rad) using *B2m* housekeeping

656 gene as an internal control.

657

Establishment of a novel *in vivo* mouse xenograft model of OSCC and oral candidiasis

659   6-8 weeks old female BALB/c mice were immuncompromised with cortisone acetate for

660   subsequent injection with human HSC-2 cells. Cortisone acetate was suspended in sterile

661   Ringer's solution containing 0.05% Tween 80 (v/v) and administered daily *per os* at a

662   concentration of 225 mg kg^{-1} [42] in a total volume of 0.2 mL using a sterile gavage (38X22G

663   curved). Because of the immunosuppression, autoclaved rodent feed and bedding were used.

664   Drinking water was supplemented with 1% 100 U/mL penicillin and 100 mg/mL streptomycin.

665   Tumor cell injection was performed on the second day. HSC-2 cells were washed twice with

666   1xPBS and trypsinized. Trypsin was then neutralized with complete growth medium, and the

667   cell suspension was centrifuged at 400xg for 5 min. After removing the supernatant, the cell

668   pellet was suspended in serum free medium. Anesthesia was performed by administration of 40

669   mg/kg pentobarbital i.p. and $1x10^6$ HSC-2 cells were injected to the apex of the tongue in 50

670   μL volume containing 10% (v/v) matrigel (Corning). Mice were continuously monitored until

671   they recovered from anesthesia.

672   Oral candidiasis was induced on the 5th day with minor modifications to the protocol described

673   previously by Solis et. al[42]. Briefly, *C. albicans* (SC5314) cells were inoculated in 5 mL YPD

674   and cultured for 24 h with continuous shaking at 30°C overnight. Inoculation and culturing was

675   performed 3 times. *Candida* cells were then washed 3 times in 1xPBS, and suspended in HBSS

676   to a concentration of $1×10^9$ cells mL^{-1}. The *C. albicans* suspension was placed in 30°C water

677   bath for 5 min. Calcium alginate swabs were placed in the suspension approximately 5 min

678   prior to use. Anesthesia was performed by administration of 40 mg/kg pentobarbital i.p.

679   Saturated calcium alginate swabs were placed under the tongues of each mouse for 75 minutes.

680   The following day, cortisone acetate was administered intraperitoneally to avoid damage in the

681   mouth. No cortisone was given at 7th and 8th day beacause cortisone acetate absorbes slower

682   through i.p. injection resulting prolonged immunosuppressive effect. The weight of the animals

683   was monitored every day. For validation of oral candidiasis, the tongue was excised and

684   homogenized for approximately 8–10 sec in PBS with a tissue homogenizer. Homogenates

685   were used for determination of fungal burdens by colony counting after plating serial dilutions

686   on YPD agar plates per tissue. The CFUs were counted after 48 h of incubation at 30°C and

687   expressed as CFU/g tissue.

688

689   **Sample preparation for sequencing from *in vivo* samples**

690   At the last day (8th) of the *in vivo* experiment mice were sacrificed and tongues were removed

691   for subsequent analyses. Mouse tongue tissues were removed from the tumor with the help of

692   scalpel. Next, 30 mg tumor tissue was homogenized (Bioneer) in RLT buffer and RNA was

693   extracted with RNeasy Plus Mini Kit (Qiagen) according to the manufacturer's instructions.

694   RNA quality and quantity were analyzed by Bioanalyzer Instrument (Agilent).

695

696   **Histopathological Analysis**

697   Mice were sacrificed and tongues were removed from the base by dissecting scissors and

698   forceps. Whole tongues were fixed in 4% formalin and kept at room temperature until specimen

699   analysis. Fixed tongues containing tumor were sectioned and stained with periodic acid-Schiff

700   (PAS) and hematoxylin-eosin (H&E) using conventional staining methods. For E-cadherin

701   staining, standard immunohistochemical procedures were applied using rabbit monoclonal

702   primary antibody (dilution: 1:200, EP700Y, Cellmarque). For vimentin staining, rabbit

703   monoclonal primary antibody (dilution: 1:300, SP20, Cellmarque) was used. For p63 staining,

704   mouse monoclonal primary antibody (dilution: 1:100, DBR16.1, Hisztopatológia Kft., Pécs,

705   Hungary) was used. Antigen retrieval was performed by epitope retrieval (ER) 2 solution

706   (Leica, pH 9). The slides were then incubated with anti-E-cadherin, anti-vimentin or anti-p63

707   antibodies for 20 min. Staining was performed with a Leica Bond Max Automatic Staining

708   System using Bond Polymer Refine Detection (Leica). The slides were mounted with coverslips

709   and assessed by microscopic examination (BX51 OLYMPUS or Zeiss Imager Z1)

710

711   **Statistical analysis**

712   Statistical analysis was performed using the GraphPad Prism 7 software. All experiments were

713   performed at least three times. Each replicate was normalized to its own control value, when it

714   was necessary, then normalized data was statistically analyzed. Paired or unpaired t-tests were

715   used to determine statistical significance (see figure legends for details) and differences

716   between groups were considered significant at p values of <0.05 (* $p \leq 0.05$; ** $p \leq 0.01$; ***

717     $p \leq 0.001$; **** $p \leq 0.0001$).

718

719

726 through projects GINOP-2.3.2-15-2016-00038 and GINOP-2.3.2-15-2016-00035 is gratefully

727 acknowledged.

728

729 **AUTHOR CONTRIBUTIONS**

730 GA and VM contributed to the concept and design of this project. VM carried out the majority

731 of experiments with the help of IN, RA, RD, VÉ, SZB, HP, TL, VC, SZA, KM, PLG. HM,

732 ASZ analyzed the acquired bioinformatics data. VM prepared the manuscript and the figures,

733 that was revised by RT, JND with AG. All authors reviewed the manuscript, contributed to the

734 discussion and approved the final version.

735

736 **DECLARATION OF INTERESTS**

737 The authors declare no competing interests.

738

739 Processed and raw expression data is available through the Gene Expression Omnibus

740 (https://www.ncbi.nlm.nih.gov/geo/) with accession number GSE169278.

741

742 **References**

743

744 1.   Markopoulos, A. K. Current aspects on oral squamous cell carcinoma. *Open Dent. J.* **6**,

745   126–130 (2012).

746 2.   Choi, S. & Myers, J. N. Molecular pathogenesis of oral squamous cell carcinoma:

747   implications for therapy. *J. Dent. Res.* **87**, 14–32 (2008).

748 3.   Global oral cancer incidence. *Br. Dent. J.* **221**, 288 (2016).

749 4.   Subapriya, R., Thangavelu, A., Mathavan, B., Ramachandran, C. R. & Nagini, S.

750   Assessment of risk factors for oral squamous cell carcinoma in Chidambaram,

751   Southern India: a case-control study. *Eur. J. cancer Prev. Off. J. Eur. Cancer Prev.*

752   *Organ.* **16**, 251–256 (2007).

753 5.   Rivera, C. Essentials of oral cancer. *Int. J. Clin. Exp. Pathol.* **8**, 11884–11894 (2015).

754 6.   Gharat, S. A., Momin, M. & Bhavsar, C. Oral Squamous Cell Carcinoma: Current

755   Treatment Strategies and Nanotechnology-Based Approaches for Prevention and

756   Therapy. *Crit. Rev. Ther. Drug Carrier Syst.* **33**, 363–400 (2016).

757 7.   Ognjenović, M. *et al.* Mucositis grades and yeast species. *Coll. Antropol.* **37**, 443–447

758   (2013).

759 8.   Reynolds, M. A. *et al.* Periodontal disease and oral microbial successions during

760   myelosuppressive cancer chemotherapy. *J. Clin. Periodontol.* **16**, 185–189 (1989).

761   9.   Sixou, J. L., De Medeiros-Batista, O., Gandemer, V. & Bonnaure-Mallet, M. The effect

762   of chemotherapy on the supragingival plaque of pediatric cancer patients. *Oral Oncol.*

763   **34**, 476–483 (1998).

764   10.   Rivera, R. E. *et al.* Characterization of oral yeasts isolated from healthy individuals

765   attended in different Colombian dental clinics. *J. Biomed. Res.* **33**, 333–342 (2019).

766   11.   Deo, P. N. & Deshmukh, R. Oral microbiome: Unveiling the fundamentals. *J. Oral*

767   *Maxillofac. Pathol.* **23**, 122–128 (2019).

768   12.   Xu, J. & Mitchell, T. G. Geographical differences in human oral yeast flora. *Clin.*

769   *Infect. Dis. an Off. Publ. Infect. Dis. Soc. Am.* **36**, 221–224 (2003).

770   13.   Cannon, R. D., Holmes, A. R., Mason, A. B. & Monk, B. C. Oral Candida: clearance,

771   colonization, or candidiasis? *J. Dent. Res.* **74**, 1152–1161 (1995).

772   14.   Berkovits, C. *et al.* Analysis of oral yeast microflora in patients with oral squamous cell

773   carcinoma. *Springerplus* **5**, 1257 (2016).

774   15.   Gadge, R., Jidewar, N. & Hande, A. Estimating the frequency of *candida* in oral

775   squamous cell carcinoma patients. *J. Datta Meghe Inst. Med. Sci. Univ.* **14**, 293–295

776   (2019).

777   16.   Sanketh, D. S., Patil, S. & Rao, R. S. Estimating the frequency of Candida in oral

778   squamous cell carcinoma using Calcofluor White fluorescent stain. *J. Investig. Clin.*

779   *Dent.* **7**, 304–307 (2016).

780   17.   Aslani, N. *et al.* Identification of uncommon oral yeasts from cancer patients by

781   MALDI-TOF mass spectrometry. *BMC Infect. Dis.* **18**, 24 (2018).

782   18.   JEPSEN, A. & WINTHER, J. E. MYCOTIC INFECTION IN ORAL

783   LEUKOPLAKIA. *Acta Odontol. Scand.* **23**, 239–256 (1965).

784   19.   Kharadi, U., Parkarwar, P., Khairnar, S., Reddy, S. & Arur, P. Clinics in Oncology

785   Oral Candidiasis Turns to Oral Cancer - A Rare Clinical. *Clin. Oncol.* **1**, 8–10 (2016).

786   20.   Sitheeque, M. A. M. & Samaranayake, L. P. Chronic hyperplastic

787   candidosis/candidiasis (candidal leukoplakia). *Crit. Rev. oral Biol. Med. an Off. Publ.*

788   *Am. Assoc. Oral Biol.* **14**, 253–267 (2003).

789   21.   Sanjaya, P. R., Gokul, S., Gururaj Patil, B. & Raju, R. Candida in oral pre-cancer and

790   oral cancer. *Med. Hypotheses* **77**, 1125–1128 (2011).

791   22.   Barrett, A. W., Kingsmill, V. J. & Speight, P. M. The frequency of fungal infection in

792   biopsies of oral mucosal lesions. *Oral Dis.* **4**, 26–31 (1998).

793   23.   Alnuaimi, A. D., Wiesenfeld, D., O'Brien-Simpson, N. M., Reynolds, E. C. &

794   McCullough, M. J. Oral Candida colonization in oral cancer patients and its

795   relationship with traditional risk factors of oral cancer: a matched case-control study.

796   *Oral Oncol.* **51**, 139–145 (2015).

797 24. Arzmi, M. H., Dashper, S. & McCullough, M. Polymicrobial interactions of Candida

798   albicans and its role in oral carcinogenesis. *J. oral Pathol. Med. Off. Publ. Int. Assoc.*

799   *Oral Pathol. Am. Acad. Oral Pathol.* **48**, 546–551 (2019).

800 25. Canković, M. & Bokor-Bratić, M. [Candida albicans infection in patients with oral

801   squamous cell carcinoma]. *Vojnosanit. Pregl.* **67**, 766–770 (2010).

802 26. Rebolledo Cobos, M. & Molina, M. *Oral pathogen Candida in patients under*

803   *antineoplastic therapies*. *Revista Facultad de Odontología* vol. 30 (2018).

804 27. Minhas, S., Kashif, M., Altaf, W. & Nagi, A. Oral Candidiasis: Complication of

805   Concomitant Chemo-radiotherapy in Patients with Oral Squamous Cell Carcinoma. *Br.*

806   *Microbiol. Res. J.* **11**, 1–11 (2016).

807 28. Jain, M. *et al.* The Oral Carriage of Candida in Oral Cancer Patients of Indian Origin

808   Undergoing Radiotherapy and/or Chemotherapy. *J. Clin. Diagn. Res.* **10**, ZC17-20

809   (2016).

810 29. Sankari, S. L., Mahalakshmi, K. & Kumar, V. N. A comparative study of Candida

811   species diversity among patients with oral squamous cell carcinoma and oral

812   potentially malignant disorders. *BMC Res. Notes* **13**, 488 (2020).

813 30. Mäkinen, A., Nawaz, A., Mäkitie, A. & Meurman, J. H. Role of Non-Albicans Candida

814   and Candida Albicans in Oral Squamous Cell Cancer Patients. *J. oral Maxillofac.*

815   *Surg. Off. J. Am. Assoc. Oral Maxillofac. Surg.* **76**, 2564–2571 (2018).

816 31. Al-Hebshi, N. N., Borgnakke, W. S. & Johnson, N. W. The Microbiome of Oral

817   Squamous Cell Carcinomas: a Functional Perspective. *Curr. Oral Heal. Reports* **6**,

818   145–160 (2019).

819 32. Paula, C. R., Sampaio, M. C., Birman, E. G. & Siqueira, A. M. Oral yeasts in patients

820   with cancer of the mouth, before and during radiotherapy. *Mycopathologia* **112**, 119–

821   124 (1990).

822 33. Epstein, J. B. *et al.* Oral complications of cancer and cancer therapy: from cancer

823   treatment to survivorship. *CA. Cancer J. Clin.* **62**, 400–422 (2012).

824 34. Stamenkovic, I. Matrix metalloproteinases in tumor invasion and metastasis. *Semin.*

825   *Cancer Biol.* **10**, 415–433 (2000).

826 35. Wei, Q., Qian, Y., Yu, J. & Wong, C. C. Metabolic rewiring in the promotion of cancer

827   metastasis: mechanisms and therapeutic implications. *Oncogene* **39**, 6139–6156

828   (2020).

829   36.   Puram, S. V *et al.* Single-Cell Transcriptomic Analysis of Primary and Metastatic

830   Tumor Ecosystems in Head and Neck Cancer. *Cell* **171**, 1611-1624.e24 (2017).

831   37.   Hasegawa, K. *et al.* YAP signaling induces PIEZO1 to promote oral squamous cell

832   carcinoma cell proliferation. *J. Pathol.* **253**, 80–93 (2021).

833   38.   Zhang, X. *et al.* Systematic analysis of genes involved in oral cancer metastasis to

834   lymph nodes. *Cell. Mol. Biol. Lett.* **23**, 53 (2018).

835   39.   Chen, C. *et al.* Gene expression profiling identifies genes predictive of oral squamous

836   cell carcinoma. *Cancer Epidemiol. biomarkers Prev. a Publ. Am. Assoc. Cancer Res.*

837   *cosponsored by Am. Soc. Prev. Oncol.* **17**, 2152–2162 (2008).

838   40.   Sasahira, T. & Kirita, T. Hallmarks of Cancer-Related Newly Prognostic Factors of

839   Oral Squamous Cell Carcinoma. *Int. J. Mol. Sci.* **19**, 2413 (2018).

840   41.   Heather L, M. K. Signaling Pathways Supporting Tumor Invasion in Head and Neck

841   Squamous Cell Carcinoma. *J. Clin. Exp. Pathol.* **05**, (2015).

842   42.   Solis, N. V & Filler, S. G. Mouse model of oropharyngeal candidiasis. *Nat. Protoc.* **7**,

843   637–642 (2012).

844   43.   Hooper, S. J., Wilson, M. J. & Crean, S. J. Exploring the link between microorganisms

845   and oral cancer: a systematic review of the literature. *Head Neck* **31**, 1228–1239

846   (2009).

847   44.   Mohd Bakri, M., Mohd Hussaini, H., Rachel Holmes, A., David Cannon, R. & Mary

848   Rich, A. Revisiting the association between candidal infection and carcinoma,

849   particularly oral squamous cell carcinoma. *J. Oral Microbiol.* **2**, (2010).

850   45.   Meurman, J., Marttila, E., Richardson, M. & Rautemaa, R. Non-Candida albicans

851   Candida yeasts of the oral cavity. *Commun Curr Res Educ Top Trends Appl Microbiol*

852   **1**, (2007).

853   46.   Weems, J. J. J. Candida parapsilosis: epidemiology, pathogenicity, clinical

854   manifestations, and antimicrobial susceptibility. *Clin. Infect. Dis. an Off. Publ. Infect.*

855   *Dis. Soc. Am.* **14**, 756–766 (1992).

856   47.   Brandt, M. E. Candida and Candidiasis. *Emerg. Infect. Dis.* **8**, 876 (2002).

857   48.   Trofa, D., Gácser, A. & Nosanchuk, J. D. Candida parapsilosis, an emerging fungal

858   pathogen. *Clin. Microbiol. Rev.* **21**, 606–625 (2008).

859   49.   Naglik, J. R., König, A., Hube, B. & Gaffen, S. L. Candida albicans-epithelial

860   interactions and induction of mucosal innate immunity. *Curr. Opin. Microbiol.* **40**,

861   104–112 (2017).

862   50.   Ye, M., Gu, X., Han, Y., Jin, M. & Ren, T. Gram-negative bacteria facilitate tumor
863   outgrowth and metastasis by promoting lipid synthesis in lung cancer patients. *J.*
864   *Thorac. Dis.* **8**, 1943–1955 (2016).

865   51.   Vargas, G. *et al.* Compositional and immunobiological analyses of extracellular
866   vesicles released by Candida albicans. *Cell. Microbiol.* **17**, 389–407 (2015).

867   52.   Westermarck, J. & Kähäri, V. M. Regulation of matrix metalloproteinase expression in
868   tumor invasion. *FASEB J. Off. Publ. Fed. Am. Soc. Exp. Biol.* **13**, 781–792 (1999).

869   53.   Sant'Anna-Silva, A. C. B. *et al.* Metabolic Profile of Oral Squamous Carcinoma Cell
870   Lines Relies on a Higher Demand of Lipid Metabolism in Metastatic Cells. *Front.*
871   *Oncol.* **8**, 13 (2018).

872   54.   Tretter, L., Patocs, A. & Chinopoulos, C. Succinate, an intermediate in metabolism,
873   signal transduction, ROS, hypoxia, and tumorigenesis. *Biochim. Biophys. Acta* **1857**,
874   1086–1101 (2016).

875   55.   Wu, J.-Y. *et al.* Cancer-Derived Succinate Promotes Macrophage Polarization and
876   Cancer Metastasis via Succinate Receptor. *Mol. Cell* **77**, 213-227.e5 (2020).

877   56.   Garcia-Bermudez, J. *et al.* Aspartate is a limiting metabolite for cancer cell
878   proliferation under hypoxia and in tumours. *Nat. Cell Biol.* **20**, 775–781 (2018).

879   57.   Liu, K. *et al.* Glyceraldehyde-3-phosphate dehydrogenase promotes cancer growth and
880   metastasis through upregulation of SNAIL expression. *Int. J. Oncol.* **50**, 252–262
881   (2017).

882   58.   Hanahan, D. & Weinberg, R. A. Hallmarks of cancer: the next generation. *Cell* **144**,
883   646–674 (2011).

884   59.   Leemans, C. R., Braakhuis, B. J. M. & Brakenhoff, R. H. The molecular biology of
885   head and neck cancer. *Nat. Rev. Cancer* **11**, 9–22 (2011).

886   60.   Rondon, A. M. R., Kroone, C., Kapteijn, M. Y., Versteeg, H. H. & Buijs, J. T. Role of
887   Tissue Factor in Tumor Progression and Cancer-Associated Thrombosis. *Semin.*
888   *Thromb. Hemost.* **45**, 396–412 (2019).

889   61.   Lo Muzio, L. *et al.* Effect of p63 expression on survival in oral squamous cell
890   carcinoma. *Cancer Invest.* **25**, 464–469 (2007).

891   62.   Goto, Y. *et al.* Possible involvement of ΔNp63 downregulation in the invasion and
892   metastasis of oral squamous cell carcinoma via induction of a mesenchymal
893   phenotype. *Clin. Exp. Metastasis* **31**, 293–306 (2014).

894   63.   Liu, S. *et al.* High Vimentin Expression Associated with Lymph Node Metastasis and
895   Predicated a Poor Prognosis in Oral Squamous Cell Carcinoma. *Sci. Rep.* **6**, 38834

896   (2016).

897   64.   Liu, L.-K. *et al.* Upregulation of vimentin and aberrant expression of E-cadherin/beta-

898   catenin complex in oral squamous cell carcinomas: correlation with the

899   clinicopathological features and patient outcome. *Mod. Pathol. an Off. J. United States*

900   *Can. Acad. Pathol. Inc* **23**, 213–224 (2010).

901   65.   Zhou, J., Tao, D., Xu, Q., Gao, Z. & Tang, D. Expression of E-cadherin and vimentin

902   in oral squamous cell carcinoma. *Int. J. Clin. Exp. Pathol.* **8**, 3150–3154 (2015).

903   66.   Sawant, S. S. *et al.* Clinical significance of aberrant vimentin expression in oral

904   premalignant lesions and carcinomas. *Oral Dis.* **20**, 453–465 (2014).

905   67.   Yuwanati, M. B., Tupkari, J. V. & Avadhani, A. Expression of E-cadherin in oral

906   epithelial dysplasia and oral squamous cell carcinoma: An in vivo study. *J. Clin. Exp.*

907   *Investig.* **2**, (2011).

908   68.   Thompson, L. D. R. Squamous cell carcinoma variants of the head and neck. *Curr.*

909   *Diagnostic Pathol.* **9**, 384–396 (2003).

910   69.   Kushwaha, S. S. *et al.* Correlation of E-cadherin Immunohistochemical Expression

911   with Histopathological Grading of Oral Squamous Cell Carcinoma. *Contemp. Clin.*

912   *Dent.* **10**, 232–238 (2019).

913   70.   Klimek-Ochab, M., Brzezińska-Rodak, M., Zymańczyk-Duda, E., Lejczak, B. &

914   Kafarski, P. Comparative study of fungal cell disruption--scope and limitations of the

915   methods. *Folia Microbiol. (Praha).* **56**, 469–475 (2011).

916